A unified parametrization of EEG.

P. J. Durka and K. J. Blinowska

April 4, 2001

Introduction

70 years since the first recording of human electroencephalogram (EEG, [1]), visual analysis of raw EEG traces is still the major clinical tool and point of reference for other methods, in spite of its inherent limitations: low repeatability and high cost.

7 years since the introduction of the matching pursuit (MP, [9]), we collected evidence suggesting that adaptive time-frequency approximation is a good candidate for a universal high-resolution parametrization of EEG, compatible with the visual and spectral analysis, and applicable to a large class of problems.

In the following we briefly discuss the need for a generally applicable method for a mathematical description (parametrization) of the signal, which would be directly related to the heritage of the traditional EEG analysis. The main section discusses in this context application of the Matching Pursuit algorithm. We present recent advances in analysis of sleep EEG and discuss earlier works on event-related potentials and epileptic recordings.

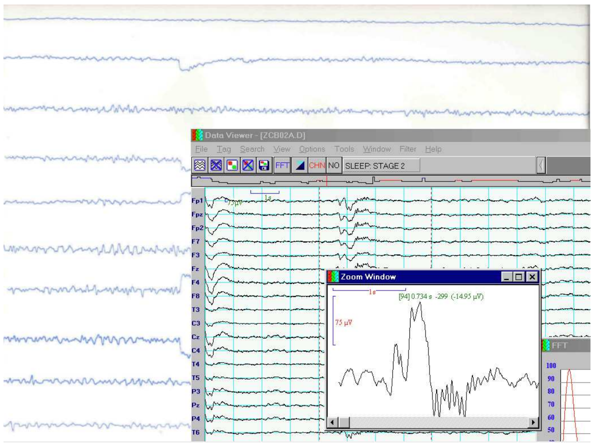

Figure 1: 70 years of progress in clinical electroencephalography: from visual analysis of EEG traces on paper (background picture) to visual analysis of EEG traces displayed on CRT (front).

Electroencephalography and science

> Every experienced electroencephalographer has his or her personal approach to EEG interpretation. (...) there is an element of science and element of art in a good EEG interpretation; it is the latter that defies standardization

…writes prof. Ernst Niedermayer in the recent edition of a fundamental reference [10]. On the contrary, physical sciences are based upon strictly repeatable experiments and unquestionable mathematical procedures. In the biomedical sciences, the experimental part is far more difficult, due to inherent inter-subject variability and the inability to control all of the experiment's conditions, especially in the studies of complex systems like the human brain. Therefore, an objective and standardized methodology of analysis is of paramount importance for the evaluation of results. Any subjective factor in the procedure of data analysis may turn the unavoidable noise into methodology-induced bias, where variation of results may reflect differences in EEG interpretation rather than inter-subject variability.

Lack of a standardized and widely accepted methodology of EEG parametrization may be one of the reasons[1] for the fact, which we would hereby

[1] At this point we should also indicate one more factor:

like to highlight: judging from the perspective of time, we can hardly notice a steady and coherent progress in the field of automatic EEG analysis. This statement may be considered controversial—however, trying to enumerate the widely accepted and applied methods of EEG analysis, it's hard to name more than:

1. visual analysis of raw EEG traces,

2. Fourier estimation of spectral power in selected frequency bands,

3. description of evoked potentials, averaged in the time domain.

In the following we'll assume that the knowledge base of EEG analysis was formed via applications of these methods. To use this indispensable experience in the clinical practice and research, on a large scale and with repeatability required by the scientific methodology, we need a generally applicable algorithm for signal description (i.e. parametrization), which would encompass the above listed approaches. But how can we relate the visual analysis to mathematics? At least a part of it can be linked with a time-frequency description. Let's consider an example from a classical reference [13]:

> The presence of sleep spindle should not be defined unless it is of at least 0.5 sec duration, i.e., one should be able to count 6 or 7 distinct waves within the half–second period. (...) The term should be used only to describe activity between 12 and 14 cps.

Mathematical implementation of such criteria allows for a scientific approach to the experience gained in decades of clinical applications, without the bias introduced by the inherent arbitrary factor, present in visual analysis. The following section presents an algorithm, which might serve as a basis for such attempt.

non-reproducible research. In an attempt to reproduce some EEG research published in a journal article, the influence of inter-subject variability may be small compared to differences in details and parameters of the applied algorithms, which are usually not published, and hence impossible to reproduce [2].

Matching Pursuit

Matching pursuit (MP) was proposed in [9] and [12]. The former publication by S. Mallat and Z. Zhang was accompanied by a freely available software implementation [8]. Below we briefly recall the basic ideas: we are looking for a linear expansion approximating the analyzed signal *s(t)*:

$$s(t) \approx \sum_{i=1}^{M} a_i g_i(t) \tag{1}$$

in terms of functions g_i chosen from a large and redundant set (dictionary D). The problem of choosing M functions, which explain the largest part of energy of a given signal, is NP-hard, i.e. computationally intractable. MP offers a sub-optimal solution, obtained by means of an iterative algorithm. In the first step of the iterative procedure we choose the vector which gives the largest product with the signal. The iterative procedure is repeated on the subsequent residua $R^n s$:

$$\begin{cases} R^0 s = s \\ R^n s = < R^n s, g_{\gamma_n} > g_{\gamma_n} + R^{n+1} s \\ g_{\gamma_n} = \arg\max_{g_{\gamma_i} \in D} | < R^n s, g_{\gamma_i} > | \end{cases} \tag{2}$$

The procedure converges to s

$$s = \sum_{n=0}^{\infty} < R^n s,\ g_{\gamma_n} > g_{\gamma_n} \tag{3}$$

and conserves signal's energy

$$||s||^2 = \sum_{n=0}^{M-1} | < R^n s,\ g_{\gamma_n} > |^2 + ||R^M s||^2 \tag{4}$$

Stochastic Gabor dictionaries

For a time-frequency parametrization, we construct the dictionary D from Gabor functions (sine modulated gaussians), which offer the lowest product of joint time-frequency spread (each dictionary contains also complete Fourier and Dirac bases). But the number of Gabor functions, which can be fitted to a given signal, is a priori infinite. Therefore in practice we restrict the dictionary D to a subset, obtained by subsampling the space of possible parameters of Gabor functions. For example, in [9] and [8] a dyadic (wavelet-like) scheme of subsampling was used.

Analyzing large amounts of sleep EEG, we encountered a statistical bias of MP decomposition, resulting from the fixed structure of the dictionary used in [8]. Since any fixed structure of a dictionary will introduce a statistical bias in the resulting MP decomposition, as a bias-free solution we proposed stochastic dictionaries [3], where the parameters of dictionary's waveforms are drawn from flat distributions.

Time-frequency distribution of energy density

We can visualize the results of MP decomposition in the time-frequency plane by adding Wigner distributions of each of the selected waveforms. The cross Wigner distribution $W[f,h](t,\omega)$ of functions f and h is defined as

$$W[f,h](t,\omega) = \int f\big(t+\frac{\tau}{2}\big)\ \overline{h\big(t-\frac{\tau}{2}\big)}\ e^{-i\omega\tau}d\tau \quad (5)$$

Calculating the Wigner distribution from the whole decomposition as defined by eq. (3) would yield

$$W[s] = \sum_{n=0}^{\infty} |<R^n s,\ g_{\gamma_n}>|^2 W g_{\gamma_n} + \sum_{n=0}^{\infty}\ \sum_{m=0,m\neq n}^{\infty} <R^n s,\ g_{\gamma_n}> \overline{<R^m s,\ g_{\gamma_m}>} W[g_{\gamma_n}, g_{\gamma_m}] \quad (6)$$

where the double sum gathers the cross terms. In a Wigner distribution of a signal, for which expansion like eq. (3) is not known, cross-terms are not explicitly separable. Minimization of their presence led to the class of Reduced Interference Distributions [14], balancing the tradeoff between resolution and cross-terms contamination. Removing cross-terms from eq. (6) is straightforward—we keep only the first sum, defining the time-frequency distribution of signal's energy as

$$Es(t,\omega) = \sum_{n=0}^{\infty} |<R^n s,\ g_{\gamma_n}>|^2\ W g_{\gamma_n}(t,\omega) \quad (7)$$

Figure 2 presents decomposition of a simulated signal (plot e, length 500 points) constructed from Gabor functions, sine wave, one-point transient and a chirp (sine with linear frequency modulation). Mentioned structures are drawn separately at the bottom of the figure (a-d). Above the signal we present time-frequency distribution of its energy calculated from the matching pursuit expansion (eq. 7). We observe clear representation of all the structures present in the signal, with exception of the chirp. Changing frequency is explained by a series of structures, since in the Gabor dictionary only waveforms of constant frequency are present.

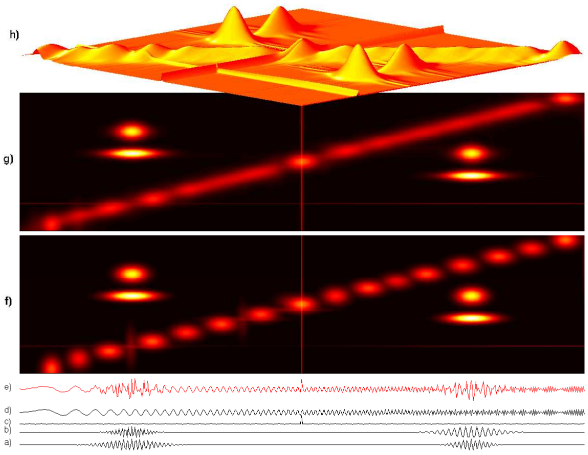

Figure 2: MP estimates of time-frequency energy distribution of a simulated 500-points signal (e) composed from Gabor functions (a, b), sine, Dirac's delta (c) and chirp (d). Plot (f) presents energy distribution (horizontal time vs. vertical frequency) constructed from a single decomposition in a large ($2{*}10^6$ atoms) dictionary. Signal is parametrized by 30 waveforms, but changing frequency of the chirp is represented as a series of Gabor functions, since in the Gabor dictionary we have only constant frequency modulations. Middle plot (g) presents average of 100 decompositions of the same signal in different realizations of smaller ($5{*}10^4$ atoms) stochastic dictionaries. This smoothes the representation of the chirp, but the underlying parametrization is not compact. Upper plot (h)—the same in 3 dimensions. Square root of energy proportional to the height of the surface or "temperature" on 2-dimensional plots.

Upper plots (g and h) of Figure 2 present an application of stochastic dictionaries, which allowed for an improved representation of changing frequency. The same signal (presented below) was decomposed 100 times in different realizations of smaller stochastic dictionary, and resulting energy distributions were averaged. Such a procedure smoothes the representation of the chirp without introducing cross-terms. However, the underlying parametrization is not compact.

Applications

Influence of drugs on sleep EEG

Three overnight EEG recordings from a double-blind test of drug influence on nocturnal sleep were subjected to:

1. Spectral analysis in the bands related to sleep spindles and slow wave activity (SWA),

2. MP decomposition in stochastic dictionaries [3].

Columns in Figure 3 present, from left to right, results for the night after administrating placebo and two sleep inducing drugs. We analyzed artifact-free data from C3–A2 derivation of the 10–20 system, sampled at 128 Hz.

Spectral estimates (rows a and c) were calculated as follows: for each 4-seconds epoch, marked by expert as artifact-free and belonging to stage II for a and stage III or IV for c, power spectral density was calculated using single Hanning window of 512 points. Red curves present the average of these estimates in the relevant frequency bands. After integrating the spectral power in these bands for each epoch, average and mean square error (indicated on the right of each plot) were calculated. For both sleep-inducing drugs we observe an increase of power in the spectral band related to sleep spindles and decrease in SWA, in agreement with the physiological expectations.

MP estimates of energy were calculated only for signal structures conforming to the generally accepted criteria for sleep spindles and SWA, based upon definitions used for standardization of visual scoring. Criteria for sleep spindles included: frequency 11–15 Hz[2], time duration 0.5–2.5 sec., peak-to-peak amplitude above 15 μV. Concordance of such selection of sleep spindles with visual detection was evaluated e.g. in [15]. Corresponding ranges of parameters for SWA were chosen as frequency 0.5–4 Hz, duration above 0.5 sec., amplitude higher than 75 μV. These structures are presented in rows b and c of Figure 3. Each of the blue dots in the frequency-amplitude coordinates marks one struc-

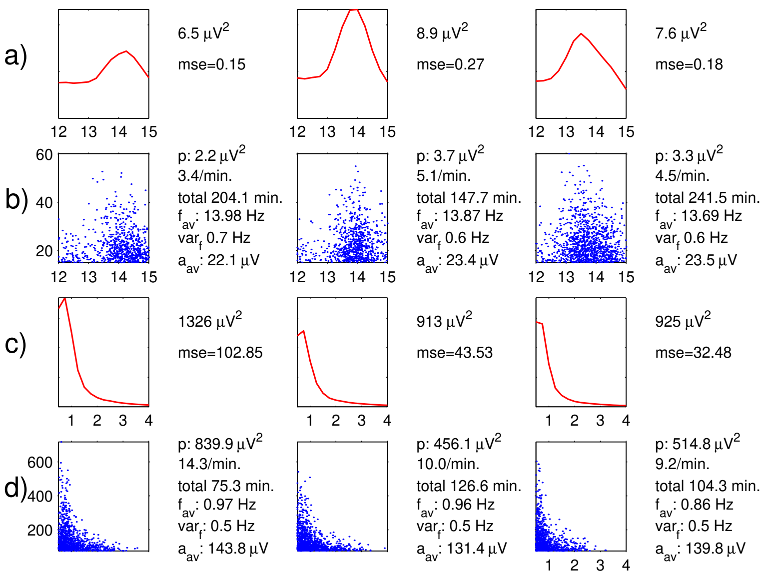

Figure 3: Analysis of sleep EEG recorded after administration of placebo (left column) and sleep-inducing drugs (middle and right columns). Rows a and c present spectra (red line) averaged in 4-sec. artifact-free epochs of stage II (sleep spindles in a) or stages III and IV (slow wave activity, SWA, in c). Numerical values on the right give the average spectral power and its mean square error. Rows b and d present structures from the MP parameterization of the same epochs, qualified as sleep spindles (b) or SWA (d). Each blue dot represents one structure of given frequency (horizontal) and amplitude (vertical), conforming to criteria set as: for sleep spindles frequency 12–15 Hz, time duration 0.5–2.5 sec., peak-to-peak amplitude above 15 μV, and for SWA frequency 0.5–4 Hz, duration above 0.5 sec., amplitude $> 75\mu V$. Parameters listed below the power include: average number of detected structures per minute, total time of qualifying EEG, average (weighted by amplitudes) frequency fav, its standard deviation v_f and average amplitude a_{av}. Data courtesy of prof. W. Szelenberger from the Medical University of Warsaw.

[2]After formulation of the classical definition from [13], it was generally agreed that the frequency range 12–14Hz is too narrow for sleep spindles.

ture detected in one of the EEG epochs, selected as for the spectral estimates above. Numbers on the right of each plot indicate their average power, average number of structures per minute, total time of artifact-free recording from qualifying stages, average frequency, its variance and the average amplitude. We observe that power estimates calculated from structures selected from MP decomposition are significantly lower than the spectral power calculated in the same frequency band. MP estimates were calculated only for structures conforming to the relevant criteria, so energy carried by unrelated waveforms, occurring in the same frequency band, was not included.

MP-based estimates proved to be more sensitive to the effects of drug influence on EEG than the spectral integrals. For the presented recordings the power of sleep spindles showed an average increase of 59% comparing to 26% increase of the spectral integrals within the same band. Average decrease of SWA power was 42%, comparing to 30% decrease of the corresponding spectral integral. Similar improvement was observed also in the other of 8 cases analyzed in this study.

Apart from the higher sensitivity, such a detailed description allows for a closer investigation e.g. of the causes of changes in the power estimates. For example, we observe from the numerical values given in Figure 3, that the change of total power of both sleep spindles and SWA results from a change in the number of their occurrences per minute rather than change of the average structure's amplitude.

Event-related desynchronization (ERD) and synchronization (ERS)

Brain's response to an external or internal stimuli can be manifested in EEG either as classical, phase-locked event-related potentials (ERP), or non-phase locked (induced) reactivity [11]. ERPs are clearly visible on the time average of properly synchronized EEG responses. On the contrary, non-phase locked activity is canceled out from the average. Classically, induced event-related desynchronization and synchronization (ERD and ERS) was quantified by the following procedure: the most reactive frequency bands were chosen by a trial-and-error procedure, and then signals, band-pass filtered within those bands, were squared before averaging (for details see [11]). This procedure not only depends on the arbitrary choice of frequency bands, but gives only an overall time course of energy of the whole band, hiding any subtle effects possibly occurring within it.

A complete structure of dynamic evolution of energy, contributing to ERD and ERS, can be calculated by averaging time-frequency distributions of single trials. As discussed above, MP offers here a high-resolution estimate, obtained from a general procedure free of a priori choices, needed e.g. for setting parameters of time-frequency distributions from the Cohen's class (see footnote 4). Detailed comparison of MP-based estimates with the classical approach, and increase of sensitivity especially in the gamma band, is discussed in [4].

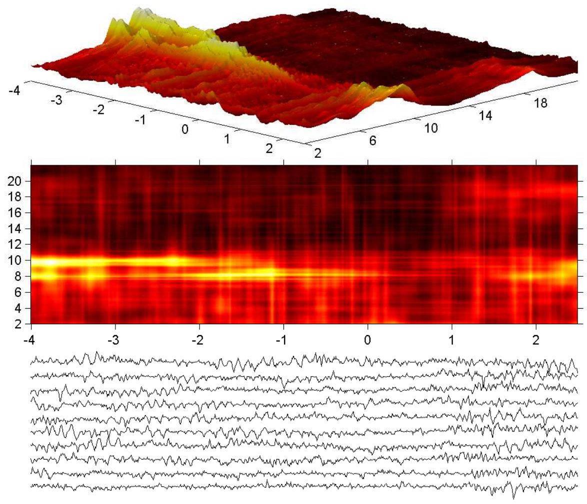

Figure 4: Bottom: first 10 of 57 EEG trials (Hjorth source derivation) recorded during a voluntary finger movement. Middle plot—average of the time-frequency distributions of energy obtained from MP parametrization. Horizontal scale in seconds (movement in time 0), vertical—frequency in Hz. Top: the same distribution in 3 dimensions, presentation as in Figure 2. We clearly observe e.g. splitting of the alpha activity into two differently reacting subbbands, a phenomenon elusive to the classical approach.

Figure 4 presents a picture of desynchronization and post-movement resynchronization in alpha and beta bands in a similar experiment concerning voluntary finger movement. Bottom plot contains time courses of 10 of 57 trials used for EEG analysis, finger movement occurring in time "0". Each trial was decomposed by MP with stochastic dictionaries ([3]), and resulting estimates of time-frequency energy density (eq. (7)) were averaged. Resulting picture is presented in two and three dimensions (middle and upper plots). We observe that two distinct alpha components are well resolved, the upper alpha desynchronizes earlier than its lower component. This example highlights advantages offered by the unique time-frequency resolution of the proposed methodology.

Time-frequency structure of epileptic seizures

Occurrence of epileptic seizures is usually visible in raw EEG, especially if recorded from intracranial electrodes (ECoG). A detailed time-frequency description can serve as a basis for their classification and for identification of different dynamic states during evolution and propagation of seizures, which was demonstrated in [6] by means of MP estimates.

Figure 5 presents one recording from [6] and time-frequency distribution of its energy, obtained by averaging decompositions in different realizations of stochastic dictionary (this procedure is presented on simulated signal in Figure 2 plots g and h). Stochastic dictionaries were not available when the original paper ([6]) was published. Their application allowed for detection of higher number of harmonics and smoother representation of changing frequencies.

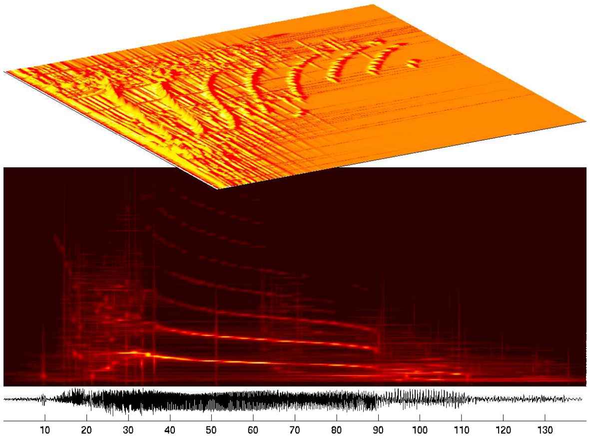

Figure 5: Bottom: intracranial recording of an epileptic seizure, horizontal axis in seconds, sampling 100 Hz. Middle time-frequency distribution of energy was obtained as follows: signal was decomposed by MP with 17 different realizations of a stochastic dictionary ($3 * 10^6$ atoms), and resulting energy distributions were averaged. Picture illustrates different dynamical states identified in [6]: near 15th second, the period of seizure initiation transforms into transitional rhythmic activity, then before 30th second the organized rhythmic activity with 8 visible harmonics becomes dominant, to dissolve into intermittent bursting activity near 90th second. Data and interpretation courtesy of prof. P. J. Franaszczuk and prof. G. K. Bergey. Top—the same distribution in 3 dimensions; presentation as in Figure 2.

Vibrotactile driving responses

Figure 6 illustrates how MP-based estimates of signal energy density (eq. 7) helped to resolve important details of spatiotemporal structure in EEG frequency-following or "driving" responses produced in somatosensory cortex by vibrotactile stimuli applied to the hand.

At the most anteromedial position (top) a small response becomes just visible between 0.5 and 1.5 s after stimulus onset. In the next two positions the main part of the response both enlarges and occurs later in the stimulus period, and in the latter it can also be seen forming just after stimulus onset. In the two most posterior and lateral recording positions the response is consistently much larger, but also breaks up progressively into two distinct phases—an early burst of activity lasting on the order of 0.5 s or less, and a later-sustained response which is sharply focused on the stimulus frequency and fills the entire second half of the stimulus period. These spatiotemporally diverse patterns are believed to reflect the differential activity of responding neural subpopulations occupying progressively shifted positions and orientations within areas 3b and 1 of primary somatosensory cortex [16].

Discussion

Mathematics behind the MP algorithm looks complicated, but to understand and use the results of the resulting parametrization equation (1) is practi-

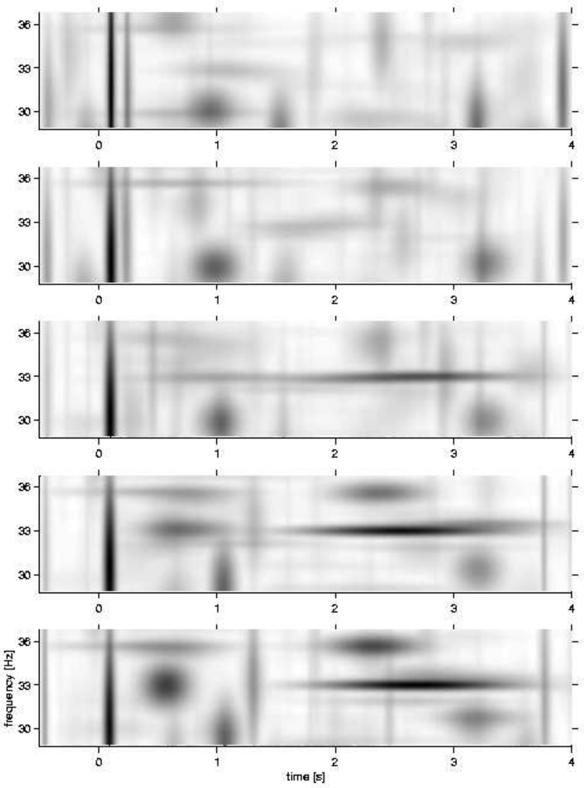

Figure 6: Energy distribution (eq. 7, proportional to shades of gray) of averaged responses to a 200 micron vibrotactile stimulus at 33Hz applied to the tip of right digit 2. Horizontal axis time in seconds, vertical—frequency between 29 and 37 Hz. The plots derive from a line of channels spanning the hand region at a spacing of 2.8 cm, with the top position anteromedial and the bottom posterolateral. The middle channel is at position C3 of the 10–20 system. Data and interpretation courtesy of prof. E. F. Kelly.

cally sufficient. In MP with Gabor dictionary, each of the functions gi from expansion (1) is characterized by the frequency and phase (of modulation), time center and width (of the Gaussian envelope), and amplitude (related to a_i from (1)). Expansion (1) can be interpreted as a parametric description of the signal's structures—at least those coherent with the dictionary.

Presented examples of MP-based analysis of sleep EEG, intracranial epileptic recordings and event-related potentials illustrate some of the advantages offered by MP parametrization of EEG[3]:

- Description of signal's structures in terms of time-frequency parameters provides a direct link to the language used for standardization of visual analysis.

- Algorithm's adaptivity to local signal's structures makes possible description of relatively weak transients (usually lost in global optimizations) and gives a high time-frequency resolution.

- MP description is also fully compatible with the Fourier transform—the second widely used method of EEG analysis (Fourier basis is a part of each dictionary used for MP decomposition).

- Due to a priori elimination of cross-terms, MP estimate of time-frequency energy distribution is robust, i.e. does not produce strong artifacts at coordinates where no activity occurs in the signal.

- MP parametrization can be used, without signal-dependent tuning of procedure's parameters[4], in a variety of problems, traditionally addressed by a variety of methods ranging from visual scoring of transients to time-frequency distributions and spectral estimates.

For a balanced picture, we should also discuss some possible drawbacks and pitfalls:

- Greedy MP algorithm requires relatively large computational resources, especially when used with stochastic dictionaries, where a priori lack of structure prevents most of the numerical optimizations [3]. However, in some cases computational complexity can be significantly reduced by a proper choice of resolutions, i.e. sizes of the dictionary, for a given problem.

[3]More detailed discussion of some of these features can be found e.g. in [3] and [5]

[4]Results given by most of the time-frequency methods depend heavily on the chosen settings, like e.g. choice of the mother wavelet, the length of time window, or various smoothing parameters governing the tradeoff between resolution and cross-terms contamination in quadratic distributions.

Rapid progress in computer technology significantly reduces the importance of computational efficiency. Finally, advances in mathematics may lead to bias-free and computationally effective algorithms.

- At present, time-frequency dictionaries are limited to structures of constant frequency and Gaussian amplitude modulation. Extensions, incorporating e.g. exponential damping or chirps, were already proposed (e.g. [7]). However, their application in EEG analysis does not seem to promise a qualitative improvement, although we'll never know until somebody really tries.

- Each derivation is analyzed separately. We'll probably have to wait at least few years for a reasonable multichannel MP, applicable in EEG research. Currently the spatial information can be retrieved by comparison of decompositions for different derivations (like e.g. in Figure 6 or [5]).

Most of the above mentioned drawbacks seem to be of transitory nature. In spite of them, MP already seems to be the best candidate for a universal method of parametrization of EEG. Description of the signal, offered by this algorithm, is suitable for analysis of both rhythmic (stationary) and transient brain activities, encompassing properties of spectral and visual EEG analysis.

Acknowledgments

Presented MP parametrization of sleep recordings was possible only owing to a long-term cooperation with prof. W. Szelenberger, dr. M. Skalski, dr. S. Niemcewicz and dr. W. Androsiuk from the Medical University of Warsaw. Epileptic EEG displayed in Figure 5 courtesy of prof. P. J. Franaszczuk and prof. G. K. Bergey from Johns Hopkins University. Figure 6 is based on data recorded by prof. E. F. Kelly from the University of North Carolina. We acknowledge the assistance of our colleagues from the Warsaw University: J. Ginter, D. Ircha and J. Żygierewicz. This work was supported by the Polish Committee for Scientific Research grant 8T11E01416.

Reproducible research

Complete software package for matching pursuit with stochastic Gabor dictionaries (with source code in C, for Unix and Windows) and visualization of results (in Java) is available from `http://brain.fuw.edu.pl/mp`.

References

[1] H. Berger. über das elektrenkephalogramm des menschen. *Arch. F. Psychiat.*, (87):527–570, 1929.

[2] J. B. Buckheit and D. L. Donoho. Wavelab and reproducible research. In A. Antoniadis and G. Oppenheim, editors, *Wavelets and Statistics*, pages 53–81. Springer-Verlag, Berlin, 1995.

[3] P. J. Durka, D. Ircha, and K. J. Blinowska. Stochastic time-frequency dictionaries for matching pursuit. *IEEE Transactions on Signal Processing*, 49(3):507–519, March 2001.

[4] P. J. Durka, D. Ircha, Ch. Neuper, and G. Pfurtscheller. Time-frequency microstructure of event-related desynchronization and synchronization. *Medical & Biological Engineering & Computing*, 39(3), May 2001.

[5] Piotr Jerzy Durka. *Time-frequency analyses of EEG.* PhD thesis, Warsaw University, Jun 1996. http://brain.fuw.edu.pl/ durka/dissert.html.

[6] P. J. Franaszczuk, G. K. Bergey, P. J. Durka, and H. M. Eisenberg. Time-frequency analysis using the matching pursuit algorithm applied to seizures originating from the mesial temporal lobe. *Electroenceph. Clin. Neurophysiol.*, 106:513–521, 1998.

[7] M. M. Goodwin and M. Vetterli. Matching pursuit and atomic signal models based on recursive filter banks. *IEEE Trans. Signal Proc.*, 47(7):1890–1902, 1999.

[8] S. Mallat and Z. Zhang. *The matching pursuit software package (mpp).* ftp://cs.nyu.edu/pub/wave/software/mpp.tar.Z.

[9] Stéphane Mallat and Zhifeng Zhang. Matching pursuit with time-frequency dictionaries. *IEEE Transactions on Signal Processing*, 41(12):3397–3415, Dec 1993.

[10] Ernst Niedermayer and F. Lopes Da Silva. *Electroencephalography: Basic Principles, Clinical Applications and Related Fields.* Williams & Wilkins, fourth edition, 1999.

[11] Gert Pfurtscheller. EEG event-related desynchronization (ERD) and event-related synchronization (ERS). In E. Niedermayer and F. Lopes Da Silva, editors, *Electroencephalography: Basic Principles, Clinical Applications and Related Fields*, pages 958–965. Williams & Wilkins, fourth edition, 1999.

[12] S. Qian, D. Chen, and K.Chen. Signal approximation via data-adaptive normalized gaussian function and its applications for speech processing. In *ICASSP-1992*, pages 141–144, March 23–26 1992.

[13] A. Rechtschaffen and A. Kales, editors. *A Manual of Standarized Terminology, Techniques and Scoring System for Sleep Stages in Human Subjects.* US Department of Health, Education and Welfare, 1968.

[14] William J. Williams. Recent advances in time-frequency representations: Some theoretical foundations. In Metin Akay, editor, *Time frequency and wavelets in biomedical signal processing*, IEEE Press Series in Biomedical Engineering, pages 1–44. IEEE press, New Jersey, 1997.

[15] J. Żygierewicz, K.J. Blinowska, P.J. Durka, W. Szelenberger, Sz. Niemcewicz, and W. Androsiuk. High resolution study of sleep spindles. *Clin. Neurophysiol.*, 110(12):2136–2147, 1999.

[16] J. Żygierewicz, E.F. Kelly, K.J. Blinowska, P.J. Durka, and S.E. Folger. Time-frequency analysis of vibrotactile driving responses by matching pursuit. *Journal of Neuroscience Methods*, 81:121–129, 1998.